JOURNAL OF VIROLOGY, Nov. 2009, p. 11341–11355 Vol. 83, No. 21
0022-538X/09/$12.00 doi:10.1128/JVI.01440-09

Human Immunodeficiency Virus Type 1 Envelope gp120-Induced Partial T-Cell Receptor Signaling Creates an F-Actin-Depleted Zone in the Virological Synapse▽†

Gaia Vasiliver-Shamis,[1] Michael W. Cho,[2] Catarina E. Hioe,[3] and Michael L. Dustin[1]*

Program in Molecular Pathogenesis, Marty and Helen Kimmel Center for Biology and Medicine, Skirball Institute for Biomolecular Medicine, New York University School of Medicine, New York, New York 10016[1]; Department of Medicine, Case Western Reserve University School of Medicine, Cleveland, Ohio 44106[2]; and Veterans Affairs New York Harbor Healthcare System, Manhattan Campus, and Department of Pathology, New York University School of Medicine, New York, New York 10010[3]

Received 13 July 2009/Accepted 25 August 2009

Cell-to-cell transmission of human immunodeficiency virus type 1 (HIV-1) occurs via a virological synapse (VS), a tight cell-cell junction formed between HIV-infected cells and target cells in which the HIV-1-infected cell polarizes and releases virions toward the noninfected target cell in a gp120- and intercellular adhesion molecule 1 (ICAM-1)-dependent process. The response of the target cell has been less studied. We utilized supported planar bilayers presenting gp120 and ICAM-1 as a reductionist model for the infected-cell membrane and investigated its effect on the target CD4 T cell. This study shows that HIV-1 gp120 interaction with its receptors is initially organized into microclusters that undergo F-actin-dependent consolidation into a central supramolecular activation complex (cSMAC). Src kinases are active in both gp120 microclusters and in the VS cSMAC. The early T-cell receptor (TCR) signaling machinery is partially activated at the VS, and signaling does not propagate to trigger Ca^{2+} elevation or increase CD69 expression. However, these partial TCR signals act locally to create an F-actin-depleted zone. We propose a model in which the F-actin-depleted zone formed within the target CD4 T cell enhances the reception of virions by releasing the physical barrier for HIV-1 entry and facilitating postentry events.

Human immunodeficiency virus type 1 (HIV-1) infection occurs most efficiently by cell contact-dependent transfer of viral particles from infected cells to noninfected target cells (23, 52, 59). Indeed, cell-to-cell transfer of HIV-1 has been shown to be up to 18,000-fold more efficient than uptake of free virions (13, 23, 65, 66). This HIV-1 transmission between CD4 T cells has been proposed to require an organized virological synapse (VS), which is an F-actin-dependent cell-cell junction enriched with HIV-1 envelope gp120 on the infected cell and with its receptors CD4 and the chemokine receptor (CKR) CCR5 (chemokine [C-C motif] receptor 5) or CXCR4 (chemokine [C-X-C motif] receptor 4) on the target cell (13, 41, 42).

We have demonstrated before that the VS can be modeled using supported planar bilayers presenting intercellular adhesion molecule 1 (ICAM-1) and HIV-1 gp120, and in this model, it resembles the immunological synapse (IS) in molecular organization (72). The IS is organized into distinct areas termed supramolecular activation complexes (SMACs) that are subdivided by their location. The central SMAC (cSMAC) contains T-cell receptor (TCR) and peptide-major histocompatibility complex, and the peripheral SMAC (pSMAC) forms a ring of lymphocyte function-associated antigen 1 (LFA-1)–ICAM-1 interactions around the cSMAC (28, 57). By comparison, in the VS, gp120 clusters in the center, forming a cSMAC, and LFA-1–ICAM-1 interactions accumulate in the pSMAC. The periphery of the IS is rich in F-actin, while the cSMAC is relatively depleted of F-actin (43, 64).

Importantly, IS formation is critical for T-cell signal integration and for coordinating migration and directed secretion (24, 37). IS formation is initiated with the generation of TCR microclusters (MCs) in the periphery, which then coalesce in an actin-dependent process to form the cSMAC. TCR-induced signaling in the context of the IS also depends upon F-actin (2, 9). TCR MCs are the sites for signaling initiation, as shown by the recruitment of active Lck, zeta chain-associated protein 70 (ZAP70), linker of activation in T cells (LAT), and Src homology 2 (SH2) domain-containing leukocyte protein of 76 kDa (SLP76) (10, 75). However, the cSMAC appears to be a central site for TCR degradation and signaling termination, as it has 20-fold-lower tyrosine phosphorylation than MCs and is enriched in lyso-bis-phosphatidic acid, a marker for multivesicular body formation and degradation (10, 71).

The most proximal event upon engagement of TCR with its cognate peptide-major histocompatibility complex is Src kinase activation (49). The two main Src kinases in T cells are Lck and Fyn, with Lck playing the dominant role in TCR signaling. Lck and Fyn phosphorylate the immunotyrosine activation motifs (ITAMs) of the CD3 chains. These phosphorylated sites serve as a docking site for ZAP70. The association of ZAP70 with the TCR complex leads to the phosphorylation of the adaptor proteins SLP76 and LAT, which in turn leads to the activation

* Corresponding author. Mailing address: Department of Pathology, Program in Molecular Pathogenesis, Skirball Institute for Biomolecular Medicine, New York University School of Medicine, 540 First Avenue, New York, NY 10016. Phone: (212) 263-3207. Fax: (212) 263-5711. E-mail: michael.dustin@med.nyu.edu.

† Supplemental material for this article may be found at http://jvi.asm.org/.

▽ Published ahead of print on 26 August 2009.

of phospholipase C γ1 (PLCγ1). PLCγ1 is phosphorylated by the interleukin-2-inducible T-cell kinase (Itk) under phosphoinositide 3-kinase (PI3K) regulation (4) and cleaves phosphatidylinositol 4,5-bisphosphate into diacylglycerol, which activates protein kinase Cθ (PKCθ), and inositol trisphosphate, leading to Ca^{2+} influx to continue the signaling cascade (58). Recruitment and activation of actin-nucleating factors by the TCR leads to actin polymerization (33). The microtubule organization center (MTOC) also polarizes toward the IS interface within minutes upon TCR signaling (29, 46, 63) to mediate directional secretion.

Aside from its critical role in initiating virus infection, the interaction of gp120 with CD4 and the CKR on target cells has also been shown to activate intracellular signaling events. Soluble gp120 and cell-free virions elicit a variety of signaling cascades in T cells and macrophages (17, 20, 47, 73), including activation of focal adhesion kinase (18, 19), Pyk2 (21), and mitogen-activated protein kinase pathway (22, 48). Soluble gp120 and cell-free virions induce Ca^{2+} influx in T cells (53) that can lead to NFAT translocation to the nucleus (16). However, the initial membrane-proximal signals triggered by gp120 in the context of the VS have never been studied. Because of the similar supramolecular rearrangements observed in the IS and the VS, we hypothesized that gp120 interaction with the target CD4 T cells activates TCR signaling machinery.

In this study, we assessed the capacity of gp120 to induce signaling in target CD4 T cells using the gp120 and ICAM-1-presenting planar bilayers to mimic the infected T-cell membrane. We monitored in real time and in fixed cells the temporal-spatial organization of signaling components. Our results demonstrate, for the first time, that similar to IS, the VS is initiated by gp120 MCs. These MCs are also the site of early activation of TCR signaling, and they ultimately converge to form the VS cSMAC. However, unlike in the IS, the early TCR signaling machinery remains partially active in the VS cSMAC, revealing a different spatial control of signaling. Importantly, an F-actin-depleted zone is formed in the VS cSMAC. Since it is known that disassembly of cortical F-actin is critical for postentry events in HIV-1 infection (74), we propose a model in which the F-actin-depleted cSMAC provides an ideal route for efficient virus entry into the target CD4 T cells.

MATERIALS AND METHODS

Cells. Activated CD4 T cells were prepared as described before (72). Briefly, human naïve CD4 T cells were purified by negative selection (Miltenyi Biotech, CA) from healthy donors (New York Blood Center, New York, NY), activated on plates coated with 5 μg/ml of anti-CD3 and anti-CD28 antibodies (BD Pharmingen, CA) for 48 h and then expanded with 100 U/ml interleukin-2 (NIH, Bethesda, MD). Cells were used for experiments 5 to 12 days postactivation.

Planar bilayers. Bilayers containing gp120 plus ICAM-1 (gp120+ICAM-1) or ICAM-1 alone were prepared and used as described before (72). Liposomes containing 12.5% Ni^{2+}-chelating 1,2-dioleoyl-*sn*-glycero-3-[*N*(5-amino-1-carboxypentyl)iminodiacetic acid]succinyl and/or glycosylphosphatidylinositol (GPI)-anchored Cy5-ICAM-1 (density of 200 to 250 mol/μm^2) were used for the bilayers. The final concentrations of 1,2-dioleoyl-*sn*-glycero-3-[*N*(5-amino-1-carboxypentyl)iminodiacetic acid]succinyl and Cy5–ICAM-1–GPI in bilayers were adjusted by the addition of dioleoylphosphatidylcholine to the liposomes. Bilayers were then prepared by applying the liposomes onto a glass coverslip of a parallel plate flow cell (Bioptechs, Butler, PA). After the bilayers were blocked with 5% casein containing 100 μM $NiCl_2$, the Ni^{2+}-chelating bilayers were incubated with His_6-tagged gp120 (from HIV-1 DH12) for 30 min at a concentration that resulted in gp120 density of 200 to 250/μm^2. The bilayers were then washed with HEPES-buffered saline containing 1% human serum albumin. The gp120 protein made in HeLa cells infected with recombinant vaccinia virus (15) was used and labeled with Alexa Fluor 488 (Invitrogen, CA). The density of Alexa Fluor 488-labeled gp120 molecules on the bilayer was determined by coating the same lipid bilayer preparations onto 5-μm-diameter silica beads and analyzing the beads by flow cytometry using fluorescein calibration beads (Bangs Laboratories Inc., IN). The ICAM-1 and gp120 densities on the bilayers were based on their expression levels on the surfaces of antigen-presenting cells and virus-infected cells, respectively (25, 72, 76). CD4 T cells were injected onto the bilayers and allowed to interact with the bilayers for the indicated times. Images were acquired either from live cells or after cells were fixed and stained.

Immunofluorescence staining. Cells were fixed with 2% paraformaldehyde, permeabilized with 0.1% Triton X-100, and stained with antibodies specific for phosphorylated Lck (phosphorylated on Y394) [pLck(Y394)] (a gift from Alan Frey, NYU School of Medicine), pSrc(Y416), total Lck, pLck(Y505), pZAP70(Y319), pLAT(Y191) pPLCγ(Y783), CD3ε, Itk, CD4 (Cell Signaling Technology), pSLP76(Y128), pCD3ζ(Y142) (BD Pharmingen), CD3ε (eBioscience), and β-tubulin (Sigma Aldrich). Following staining with the primary antibody, the appropriate Alexa Fluor 546-labeled secondary antibody (Invitrogen, CA) was added. F-actin was detected with Alexa Fluor 568-phalloidin (Invitrogen, CA).

Treatment with anti-gp120 MAbs, CKR antagonists, and Lck inhibitor. Anti-gp120 monoclonal antibodies (MAbs) were obtained from Susan Zolla-Pazner (NYU School of Medicine) and James Robinson (Tulane University). Bilayers were treated with 20 μg/ml of the MAb for 30 min prior to introduction into the cells. The cells were also suspended in buffer containing 20 μg/ml of the same MAb before injection onto the bilayer. AMD-3100 and TAK-779 were used at 10 μM to treat the cells. These CKR antagonists were added to the cells for 30 min prior to injection onto the bilayer and kept throughout the experiment.

The Lck inhibitor (compound number 43) was a gift of M. Brown (Boehringer-Ingelheim Pharmaceuticals Inc., CT) (32) and used at the indicated concentrations. Cells were pretreated with the Lck inhibitor for 30 min prior to injection onto the bilayer and kept throughout the experiment. The control cells in experiments with CKR antagonist and Lck inhibitor experiments were treated with dimethyl sulfoxide (DMSO).

Ca^{2+} analysis. Cells were labeled with 5 μM Fura-2 (Invitrogen) and introduced onto the bilayers. Images were acquired for a total of 60 min in 30- to 60-s intervals. Calcium influx was measured using Improvision Volocity software (Waltham, MA). The ratio between Fura-2 intensity at 340 nm/380 nm in cells contacting the bilayer (as determined by interference reflection microscopy [IRM] channel) was measured over time to detect changes in intracellular Ca^{2+} levels. Ionomycin (1 μM) was added at the end of the experiment as a positive control, while the subsequent addition of 2 mM EGTA measured Ca^{2+} basal levels.

Microscopy. Multicolor fluorescence microscopy and IRM (38) were performed on an automated microscope with an Olympus total internal reflection fluorescence microscopy (TIRFM) module (62) and an Orca-ER cooled charge-coupled-device (CCD) camera or electron multiplier (EM)-CCD camera (Hamamatsu). The hardware on the microscope was controlled using Scanalytics IP-Lab software (Rockville, MD) on a Dell personal computer. Solamere Technology (Salt Lake City, UT) provided integration support.

Image analysis. Image processing and bilayer calibration were performed with IP-Lab and Metamorph software. Measurement of signaling in the cSMAC was done by determining fluorescence intensity in the cSMAC area marked by gp120 fluorescence accumulation. Measurement of signaling molecules in cells on the control ICAM-1 bilayers was done on the entire cell-bilayer contact area as detected in the IRM channel (72). Average fluorescence intensity was measured using Metamorph software in each of the areas designated above. The background fluorescence was subtracted from the average intensity. The integrated fluorescence intensity was then calculated by multiplying the average intensity by the total pixel area measured in each cell. The pixel area was converted to μm^2 based on the pixel/μm^2 ratio for the specific cameras and objectives that were used.

Statistics. Statistical analyses were done with one-way analysis of variance test and Dunn's multiple-comparison posttests or with Mann-Whitney *t* test using the GraphPad Prism software (San Diego, CA).

RESULTS

Generation of the virological synapse and initiation of signaling. We employed TIRFM on T cells forming VSs on bilayers containing gp120 and ICAM-1 to investigate whether the VS SMACs are assembled from MCs and whether the

SMACs and MCs are associated with active signaling components. Throughout this study, we used in vitro-activated primary human CD4 T cells. We visualized CD4 T cells interacting with bilayers containing gp120 plus ICAM-1 using an EM-CCD camera at a magnification of ×150 (pixel size of 125 nm). gp120 MCs were formed on the periphery of cell-bilayer contact areas within 30 s, and by 5 to 6 min, they coalesced to form a cSMAC (Fig. 1A) (see movie S1 in the supplemental material). While we had previously observed the gp120 cSMAC (72), this is the first time that gp120 MCs have been observed. We measured integrated and average fluorescence intensity levels of gp120-positive structures (Fig. 1B). The integrated fluorescence intensity is the sum of intensity values for all pixels in the gp120-positive area in each cell, while the average fluorescence reflects the intensity value per pixel in the gp120-positive area. From the integrated intensities, three phases were observed in gp120 interaction: a lag phase for the first 3 min, a steep increase from 3 to 5 min, and a plateau after 5 min. This result is consistent with the observation that individual gp120 MCs were formed mainly during the first 5 min and the MCs subsequently converge into a cSMAC. In contrast, the average intensity reaches a maximum level in less than a minute, indicating that the density of gp120 needed to form a MC is close to the saturated level for gp120 per unit area of membrane. The fluorescence intensity of individual gp120 MCs at 0 to 6 min (Fig. 1C) and cSMAC at 9 to 11 min (Fig. 1D) was plotted as a function of size to show that indeed there was no correlation between the increase in intensity and the size of gp120 MCs or the cSMAC (R^2 values of 0.0184 and 0.03783 for MCs and cSMAC, respectively). This strengthens the notion that the cSMAC is formed by convergence of saturated gp120 MCs. In this respect, gp120 MC resembles TCR MC in their behavior, as the average intensity of TCR MC also does not increase as they fuse with each other and move to the center to form the IS cSMAC (R. Varma et al., unpublished results).

We next determined whether MC convergence to form a cSMAC was F-actin dependent. We observed that gp120 MC formation was dependent on F-actin, as treatment of cells with latrunculin A (latA) prior to injection onto the bilayers resulted in no MC formation (data not shown). When latA was added to cells at 2 min, after nascent VS was formed and initial spreading was complete, gp120 MCs lost their intensity over time and disassembled (Fig. 1E) (see movie S2 in the supplemental material), indicating that once formed, the gp120 MCs were still actin dependent. As expected, latA also prevented cluster movement and cSMAC formation (Fig. 1E) (see movie S2 in the supplemental material). In contrast, the cSMAC was found to be F-actin independent, as latA treatment had no effect when added at 10 min (Fig. 1F) (see movie S3 in the supplemental material). The early F-actin dependency is consistent with a previous report showing lack of VS formation upon actin inhibition (41), but this study further shows that once formed, VS cSMACs become F-actin independent.

Next we sought to determine whether signaling was associated with gp120 MCs. CD4 T cells were introduced onto bilayers containing gp120+ICAM-1 and were fixed at 5 min (Fig. 2A) or 30 min (Fig. 2B) and then stained with an antibody recognizing the activation loop of Src kinase [pSrc(Y416)]. This antibody recognizes the activation loops of both Lck and Fyn. Images of cell-bilayer contacts were acquired using TIRFM, which detects fluorescence within 100 to 200 nm from the interface and increases the signal-to-noise ratio, enabling the detection of VS proximal signaling events. Activated Src kinases were found in the VSs in association with gp120 MCs (Fig. 2A). Interestingly, active Src kinase staining remained intense in the cSMAC (Fig. 2B). In fact, pSrc(Y416) average intensity in the cSMAC at 30 min was slightly higher than the intensity associated with the individual MCs at 5 min, although the intensities of some individual clusters were similar to that of the cSMAC (Fig. 2C). pSrc(Y416) staining in cells on ICAM-1 bilayers showed no MCs (data not shown). There was only a slight, insignificant, increase in pSrc(Y416) integrated intensity in the cSMAC between 5 and 30 min (Fig. 2D), indicating that the Src activation does not increase after the cSMAC assembles. Since there was no significant difference in the level of Src phosphorylation in gp120 MCs compared to cSMAC, we decided to focus on the signaling events taking place in the cSMAC.

Lck, but not Fyn, is the active Src kinase in the VS. We further investigated which was the active Src family kinase in the VS. CD4 T cells interacting with gp120+ICAM-1 or ICAM-1 bilayers for 45 min were fixed and stained with antibodies specific for pLck as well as total Lck and Fyn. We chose a single time point (45 min) for this analysis, since no substantial differences in the levels of Src activation were observed at early or late time points during the VS formation (Fig. 2C and D). Moreover, at 45 min, active signaling is completely extinguished in the IS cSMAC, allowing us to evaluate differences in spatiotemporal signaling in the IS versus the VS. The ICAM-1 bilayer served as a control to indicate the basal levels of the active signaling components and the levels that can be induced by outside-in integrin signaling. Throughout this study, specific fluorescence intensity was measured within the cSMAC for cells on gp120+ICAM-1 bilayers (Fig. 3A, top panel, dashed yellow line) and within the whole contact area for cells interacting with the ICAM-1 bilayer (Fig. 3A, bottom panel, dashed yellow line). An increase of average fluorescence intensity reflects the increased recruitment and activation of the signaling molecule to the VS interface, and this will be confirmed by a similar increase in the integrated fluorescence intensity. In contrast, no change in the integrated fluorescence intensity indicates a redistribution of the signaling molecule.

After the cells interacted with gp120+ICAM-1 bilayers, total Lck, pLck(Y394), and pLck(Y505) were all recruited to the VS interface and were highly colocalized with gp120 (Fig. 3A, B, and C, respectively). The average intensity of total Lck (Fig. 3A, left graph) was higher on the gp120+ICAM-1 bilayer than on the ICAM-1 bilayer, but the integrated intensity levels (Fig. 3A, right graph) were similar, suggesting that Lck is redistributed into a central cluster upon CD4 binding to gp120. However, quantification of pLck(Y394) (Fig. 3B, left graph) showed that the average intensity on gp120+ICAM-1 bilayers was more than 10-fold higher than that on ICAM-1 bilayers, and the integrated intensity was 2-fold higher on gp120+ICAM-1 bilayers than on ICAM-1 bilayers (Fig. 3B, right graph). This indicates that while the levels of total Lck at the interface are similar in cells adhering onto gp120+ICAM-1 and ICAM-1 bilayers, gp120 binding increased phosphorylation of the Lck activation loop.

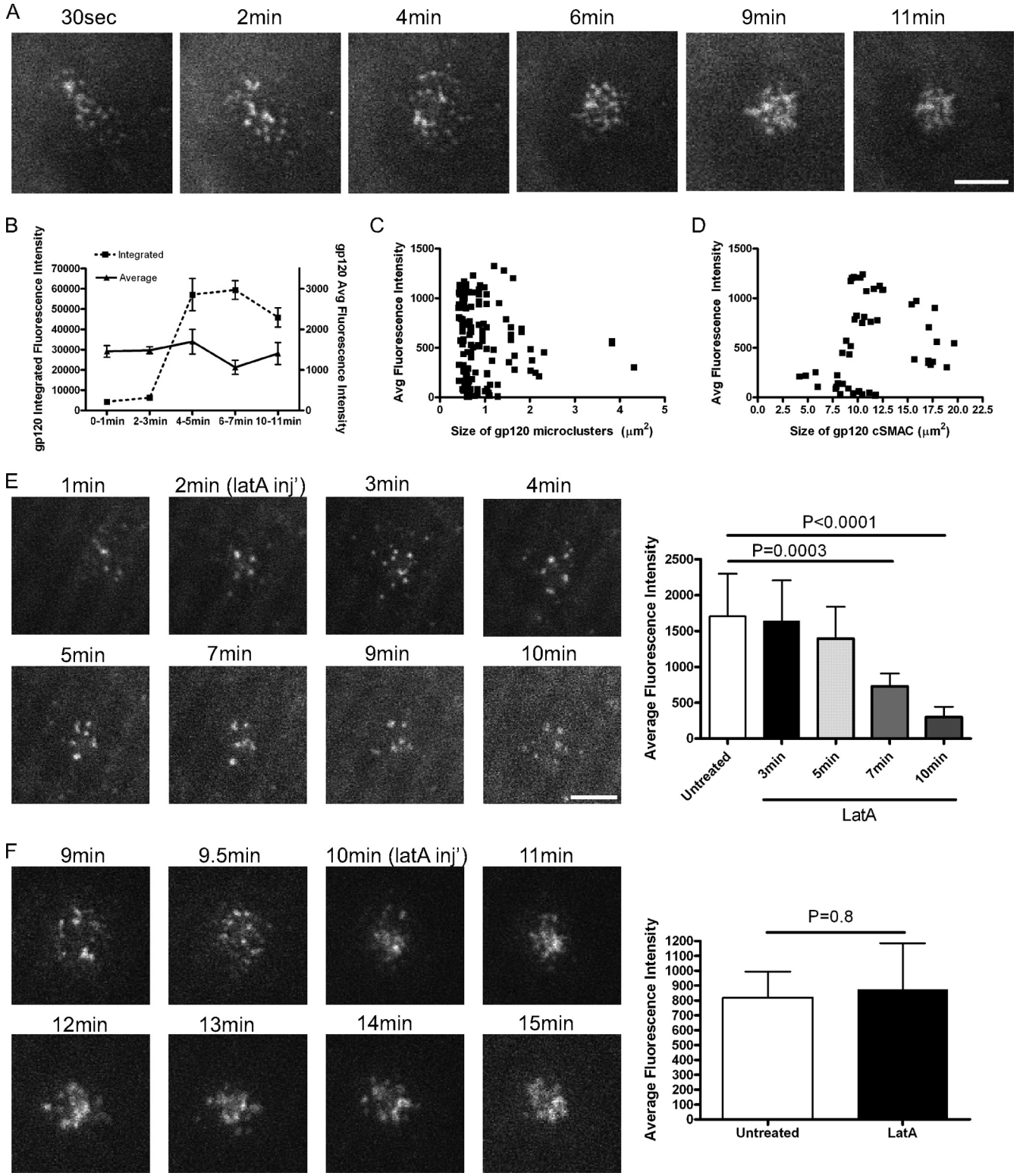

FIG. 1. HIV-1 gp120 MCs at the initiation of HIV-1 VS assembly. (A) Activated CD4 T cells were introduced onto gp120+ICAM-1 bilayers. The same fields were imaged continuously for 12 min. Representative images depicting gp120 MCs at the indicated times are shown. (B) Quantification of integrated and average fluorescence intensities ± standard errors of the means (error bars) of gp120 clusters over time. The average values from three independent experiments are shown. Twenty VSs were analyzed in each experiment. (C and D) Average fluorescence intensity of gp120 MCs (C) or VS cSMAC (D) as a function of size. Data shown are from one representative experiment out of three independent experiments. CD4 T cells were introduced onto gp120+ICAM-1 bilayers. (E and F) The same fields were imaged for 10 min (E) or 15 min (F). 1 μM latA was added at 2 min (E) or 10 min (F) (latA inj', latA injected). Representative images of one cell at designated time points before and after latA treatment are shown. Graphs showing average fluorescence intensities plus standard deviations (error bars) of gp120 MCs at the different time points are also shown next to the images in panels E and F. Data are from one representative experiment out of two independent experiments. Fifteen to twenty synapses were analyzed for each experiment. Bars = 5 μm.

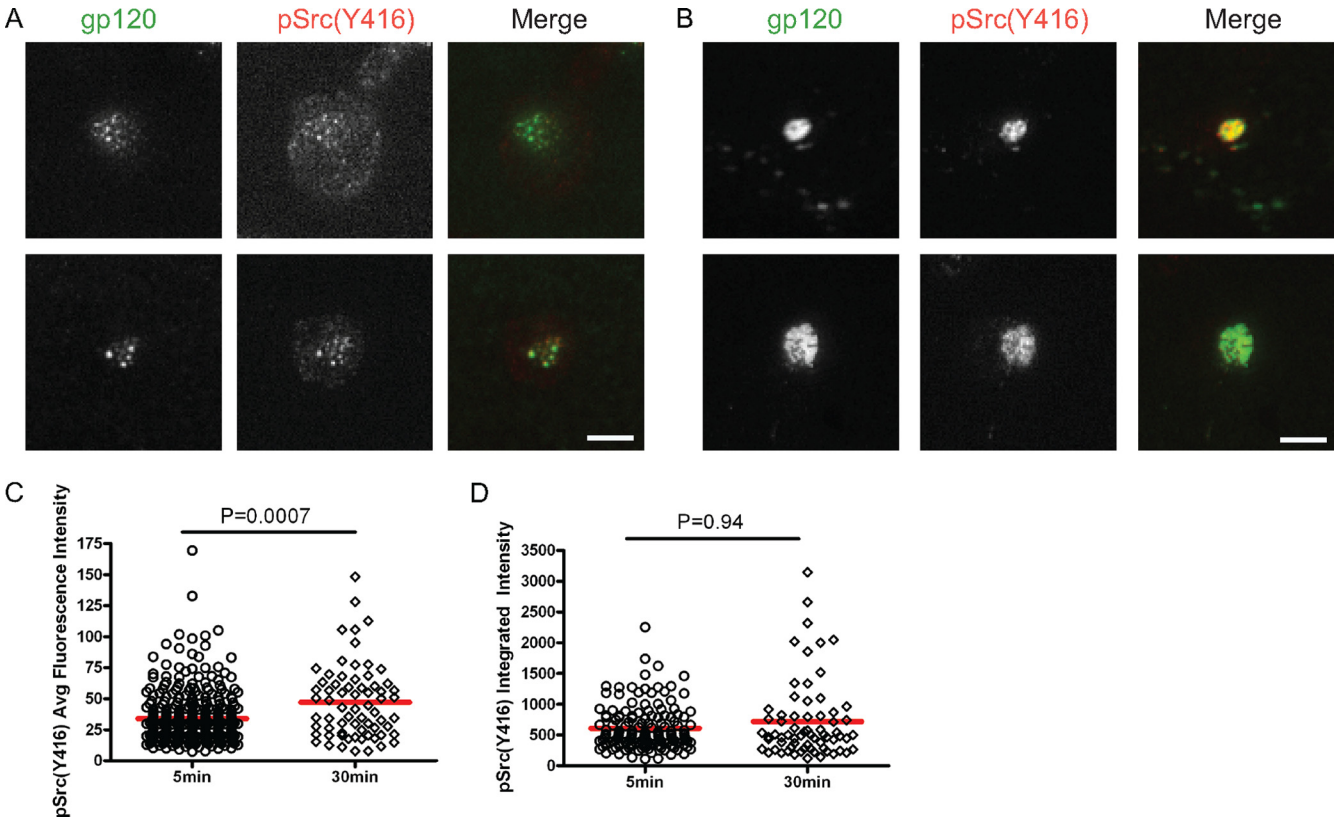

FIG. 2. Src phosphorylation associated with gp120 clustering. (A and B) Activated CD4 T cells were introduced onto gp120+ICAM-1 bilayers for 5 min (A) or 30 min (B) and then fixed and stained with a phospho-Src(Y416)-specific antibody. Representative images for the two different time points are shown. (C and D) Average and integrated intensities of pSrc(Y416) associated with the gp120 MCs at 5 min and with the cSMAC at 30 min. Data shown in panels C and D are from one out of two independent experiments. Bars = 5 μm.

Additionally, staining for the inhibitory C-terminal phosphorylation site of pLck(Y505) showed a >20-fold increase in average intensity (Fig. 3C, left graph) and a 3-fold increase in integrated intensity (Fig. 3C, right graph) for cells on gp120+ICAM-1 bilayers compared to cells on ICAM-1 bilayers. Thus, the increase in activation loop phosphorylation appears to be counterbalanced by phosphorylation of the inhibitory C-terminal phosphorylation site. It is not clear whether this pattern reflects the presence of two populations of Lck enzymes with mutually exclusive phosphorylation of positions 394 and 505 or if some Lck in the VS are phosphorylated on both sites (60). In contrast, Fyn was not recruited to the VS (Fig. 3D), and significantly more Fyn was recruited to the contact area of cells on ICAM-1 bilayers than on gp120+ICAM-1 bilayers, possibly due to integrin outside-in signaling (14). From these data, we conclude that Lck, but not Fyn, is the active Src kinase in the VS.

Next, we investigated the importance of gp120 interactions with its receptors for Lck activation. CD4 cross-linking by antibodies is sufficient to induce Lck activation (35). Blocking gp120-CD4 interaction by MAb 654 reduced Lck phosphorylation by 85% based on measurement of average fluorescence intensity by TIRFM (Fig. 3E). The importance of gp120-CD4 binding is also supported by the observation that CD4 localized to the gp120 contact areas in cells on gp120+ICAM-1 bilayers (Fig. 4A). Intriguingly, blocking gp120-CKR interaction by MAb 2219, which binds to the V3 loop involved in CKR binding, led to a 40% increase in pLck(Y394) levels compared to control (Fig. 3E). Similarly, blocking CXCR4 and CCR5 by the respective small CKR antagonists AMD-3100 and TAK-779 lead to 30% to 80% increase in active Lck compared to the control, and blocking both CKRs led to 200% increase in pLck(Y394) levels (Fig. 3F). Hence, Lck activation in the VS is CD4 dependent and may be negatively regulated by gp120-CKR interaction.

Involvement of the TCR-CD3 complex in the VS. The TCR signaling cascade involves Lck phosphorylation of CD3 ITAMs; therefore, we next determined whether the TCR-CD3 complex was recruited to the cSMAC in the target cell. Although Jolly et al. (41) indicated the absence of TCR in the VS, partial enrichment of CD3ε was found at the VS interface in a small fraction (15%) of cell-cell conjugates analyzed, and the other subunits of the TCR-CD3 complex were not evaluated. Hence, we determined whether the different subunits of the TCR-CD3 complex were recruited in the target cell. The alpha and beta subunits of TCR (αβTCR) were concentrated in the cSMAC (Fig. 4B) of cells on gp120+ICAM-1 bilayers compared to the average intensity of cells on ICAM-1 bilayers, but the integrated αβTCR signals over the respective interfaces were similar. This is indicative of redistribution of the αβTCR from the interface to the gp120 cluster. CD3ε was also present in the VS at higher levels compared to cells on the ICAM-1 bilayer (Fig.

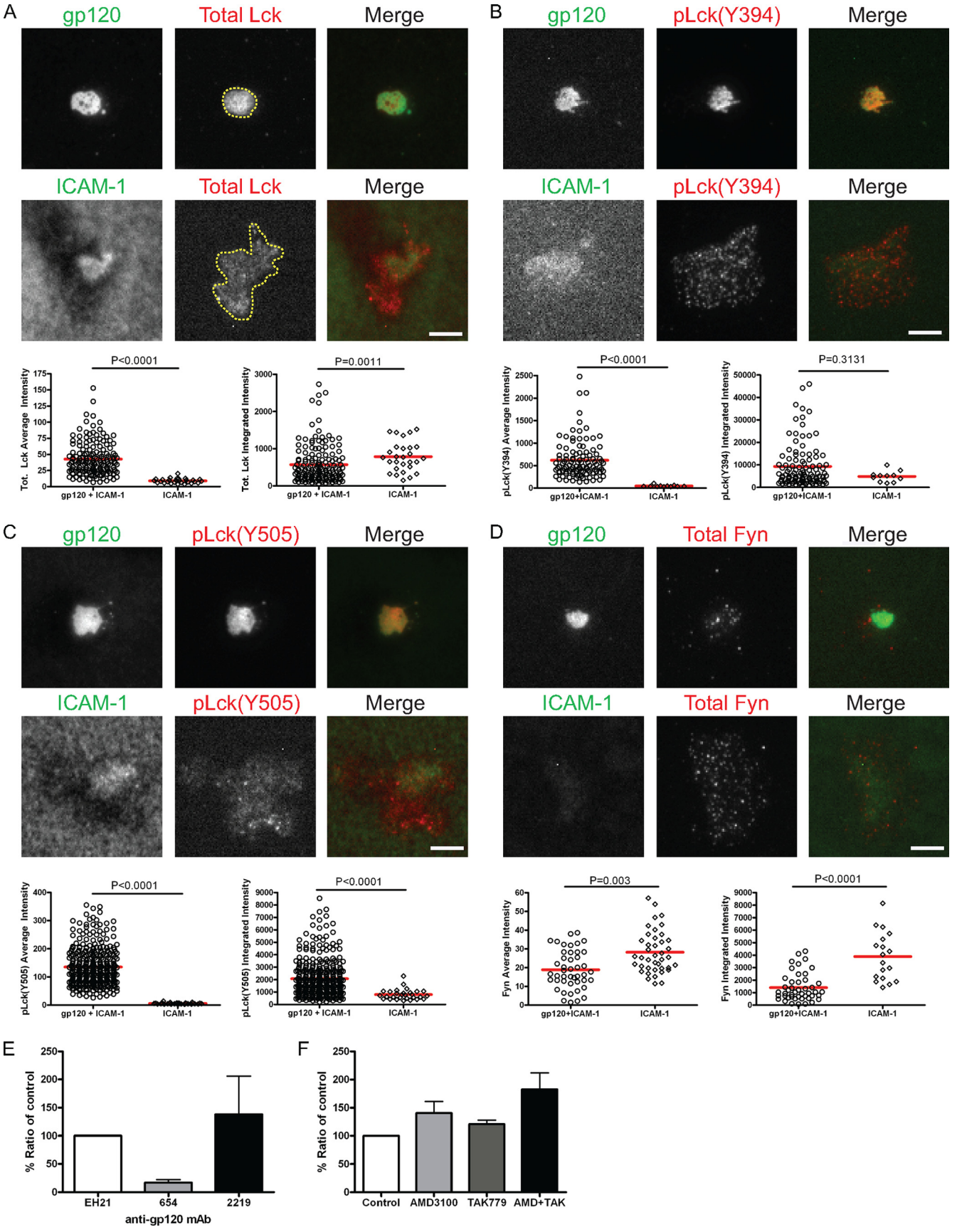
A
gp120
Total Lck
Merge
ICAM-1
Total Lck
Merge
P<0.0001
Tot. Lck Average Intensity
gp120 + ICAM-1
ICAM-1
P=0.0011
Tot. Lck Integrated Intensity
gp120 + ICAM-1
ICAM-1
B
gp120
pLck(Y394)
Merge
ICAM-1
pLck(Y394)
Merge
P<0.0001
pLck(Y394) Average Intensity
gp120+ICAM-1
ICAM-1
P=0.3131
pLck(Y394) Integrated Intensity
gp120+ICAM-1
ICAM-1
C
gp120
pLck(Y505)
Merge
ICAM-1
pLck(Y505)
Merge
P<0.0001
pLck(Y505) Average Intensity
gp120 + ICAM-1
ICAM-1
P<0.0001
pLck(Y505) Integrated Intensity
gp120 + ICAM-1
ICAM-1
D
gp120
Total Fyn
Merge
ICAM-1
Total Fyn
Merge
P=0.003
Fyn Average Intensity
gp120+ICAM-1
ICAM-1
P<0.0001
Fyn Integrated Intensity
gp120+ICAM-1
ICAM-1
E
% Ratio of control
EH21
654
2219
anti-gp120 mAb
F
% Ratio of control
Control
AMD3100
TAK779
AMD+TAK

4C), but it mainly localized to the pSMAC area. In contrast, CD3ζ phosphorylation was strongly induced in cells on gp120+ICAM-1 bilayers, and active CD3ζ highly colocalized with gp120 (Fig. 4D). This was confirmed by quantification of the average and integrated intensities of pCD3ζ(Y142) (Fig. 4D, graphs). The same results were obtained when another phospho-specific CD3ζ antibody was used (data not shown). Hence, specific components of the TCR-CD3 complex were recruited to the VS, and CD3ζ was highly phosphorylated.

Recruitment and activation of ZAP70, LAT, SLP76, and PLCγ in the VS. The phosphorylated CD3ζ chain in the VS suggests that signaling may propagate downstream. To explore this, we examined the well-characterized TCR signaling components, i.e., ZAP70, LAT, SLP76, and PLCγ by staining with phospho-specific antibodies for the active molecules. pZAP70(Y319) colocalized with gp120, and its average intensity was 12-fold higher in cells on gp120+ICAM-1 bilayers than in cells on ICAM-1 bilayers (Fig. 5A). pLAT(Y191) also colocalized with gp120 in the VS, with a 16-fold increase in average intensity (Fig. 5B). Similarly, pSLP76(Y128) was recruited to the VS, with an average intensity 20-fold higher on gp120+ICAM-1 bilayers than onICAM-1 bilayers (Fig. 5C). Furthermore, pPLCγ(Y783) was recruited specifically to the VS cSMAC (Fig. 5D). All together, our data show that a signaling cascade is initiated at the HIV-1 gp120-induced VS by exploiting the TCR signaling machinery.

Absence of canonical T-cell activation in the VS. Since we found active PLCγ in the VS, we investigated whether Ca^{2+} influx was induced. CD4 T cells labeled with Fura-2 were introduced to the bilayers and imaged over 70 min, followed by injections of ionomycin and EGTA. Ca^{2+} levels were similar in cells on gp120+ICAM-1 and ICAM-1 bilayers (Fig. 6A). This result was confirmed using alternative Ca^{2+}-sensing dyes Fluo-4 and Fluo-Lojo (data not shown). We also did not observe PKCθ recruitment to the VS interface (data not shown). Moreover, we detected no significant increase in CD69 expression in cells interacting with gp120+ICAM-1 bilayers compared to cells on ICAM-1 bilayers (data not shown). These data indicate that the signaling induced in the VS does not lead to full canonical T-cell activation.

VS induces partial activation of Akt. As HIV-1 infection is tightly linked to target cell activation, we examined the PI3K/Akt signaling pathway that promotes cell survival and metabolism. Itk was recruited to the VS interface (Fig. 6B), implying that PI3K is activated in the VS. We then evaluated Akt activation that resulted from phosphorylation of its T308 residue by phosphoinositide-dependent kinase 1 (PDK1). TIRFM revealed phosphorylation of Akt on T308 in the cSMAC with an intensity twofold greater on gp120+ICAM-1 bilayers than on ICAM-1 bilayers (Fig. 6C). In contrast, no significant difference was observed in phosphorylation of Akt on S473 (phosphorylated by mTOR [mammalian target of rapamycin]) between cells on gp120+ICAM-1 or ICAM-1 bilayers (Fig. 6D). Since mTOR is central to metabolic changes associated with increased survival of T cells (5), there is no evidence for complete prosurvival signaling within the target cell.

Cytoskeleton rearrangement in the VS. We next investigated the pattern of F-actin in the VS. We stained fixed cells with Alexa Fluor 568-phalloidin to detect F-actin. Intact VSs displayed peripheral F-actin accumulation with relative depletion at the center (Fig. 7A, top panels). After the VSs disassembled and the cells resumed migration, actin was enriched in the leading lamellipodium (Fig. 7A, bottom panels). The F-actin integrated fluorescence intensity was about sixfold higher in pSMAC compared to cSMAC (Fig. 7B), supporting the notion that the VS cSMAC is depleted of F-actin.

In the VS, MTOC polarized (Fig. 7C, top panels) to the center only in 30% of the cells, and in a similar portion of the cells (25%), no polarization was observed (Fig. 7C, middle panels). The remaining cells were migratory, and the MTOC was located at the uropod (Fig. 7C, bottom panels). The percentages of cells exhibiting distinct MTOC polarization are shown in Fig. 7D; there was no significant difference among the three groups ($P = 0.1$). Thus, the cSMAC marks an F-actin-depleted central zone that does not strongly recruit the MTOC.

Lck signaling is required for VS-induced actin rearrangement. To evaluate whether the signaling induced in the VS was required for formation of an F-actin-depleted zone, we utilized an Lck-specific inhibitor. Treatment of CD4 T cells with 2 to 200 μM Lck inhibitor prior to introduction to gp120+ICAM-1 bilayers resulted in 86 to 94% decrease in pLck(Y394) levels at the VS interface (Fig. 8A). Since 2 μM Lck inhibitor treatment was sufficient to block Lck activation, we continued working with this concentration. Next we examined the effect of Lck inhibition on actin polymerization by treating the cells with the Lck inhibitor and detecting F-actin with Alexa Fluor 568-phalloidin. The Lck inhibitor did not affect VS formation, and a cSMAC was formed similar to that observed in the control cells that were treated with DMSO (Fig. 8B). However, an F-actin-depleted zone was not formed when Lck was inhibited (Fig. 8B). In fact,

FIG. 3. Lck activation in the VS and its dependence on gp120-CD4 interaction. CD4 T cells were introduced onto bilayers containing gp120 and ICAM-1 or ICAM-1 alone for 45 min and then fixed and stained for total Lck (A), pLck(Y394) (B), pLck(Y505) (C), and total Fyn (D). Images of representative cells on the gp120+ICAM-1 bilayer (top panels) and the ICAM-1 bilayer (bottom panels) are shown. Fluorescence intensities of the individual cells were quantified within the areas marked with the yellow dashed lines in panel A. Quantification of average and integrated intensities detected by TIRFM are presented in the left and right graphs, respectively. A total of 30 to 350 cells were quantified for each condition. Comparable data were obtained from three independent experiments; data from one experiment are presented. Bars = 5 μm. (E) CD4 T cells were introduced onto gp120+ICAM-1 bilayers in the presence of an anti-gp120 MAb that blocks gp120-CD4 interaction (MAb 654), an anti-V3 MAb that interferes with gp120 interaction with the CKR (MAb 2219), or a control MAb to the N terminus of gp120 that does not affect gp120 binding to its receptors (MAb EH21). The MAbs were used at 20 μg/ml. (F) CD4 T cells were pretreated with 10 μM of CKR antagonist AMD-3100 or TAK-779 or both and then introduced onto gp120+ICAM-1 bilayers in the presence of antagonists. Cells were fixed and stained for pLck(Y394). The average fluorescence intensity detected by TIRFM was measured and presented as a percentage of control plus standard error of the mean (error bar). Data shown in panels E and F are average values from three independent experiments.

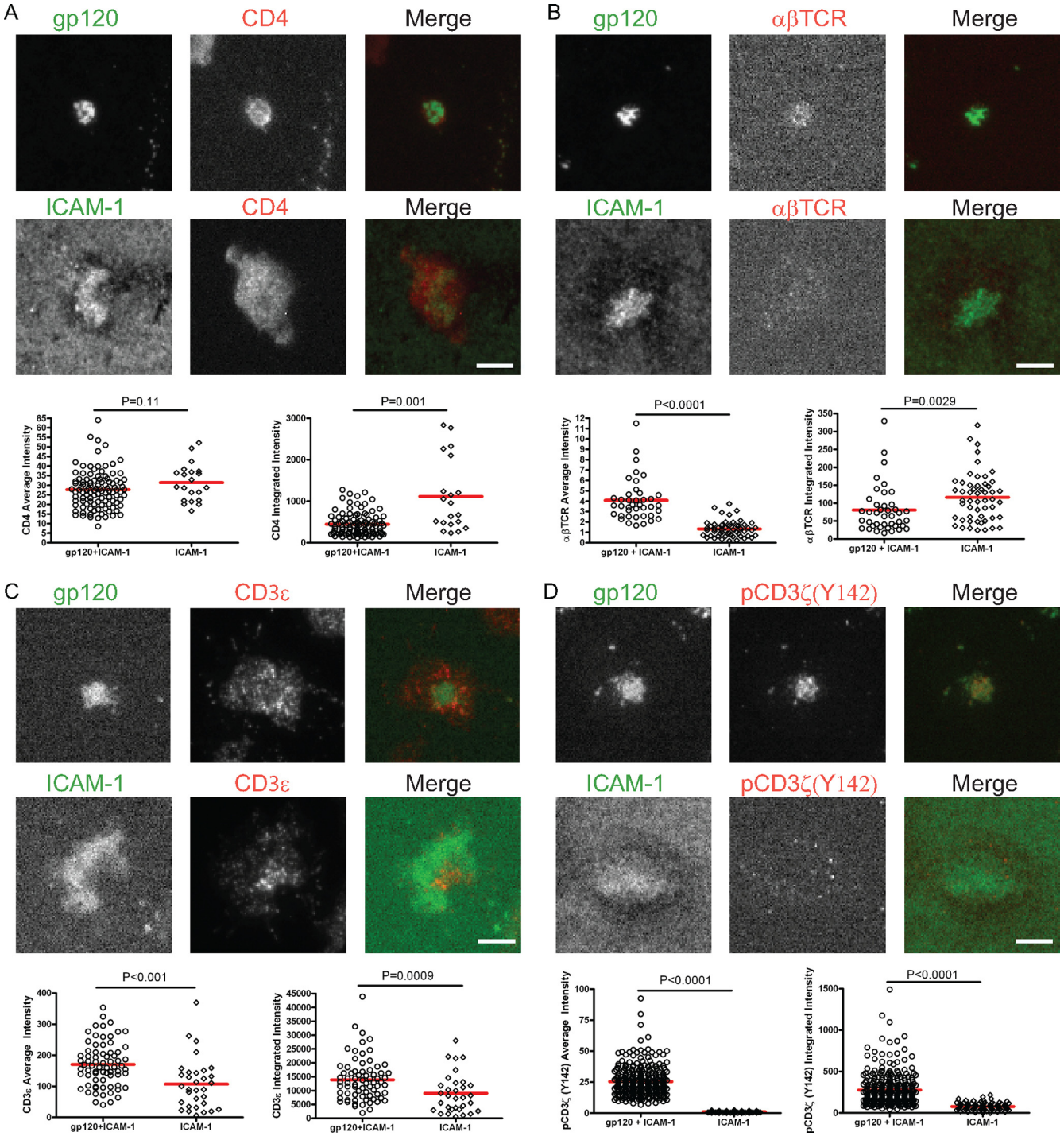

FIG. 4. CD4 localization and TCR-CD3 involvement in the VS. CD4 T cells interacted with gp120+ICAM-1 or ICAM-1 bilayers for 45 min and then were fixed and stained for CD4 (A), αβTCR (B), CD3ε (C), and pCD3ζ(Y142) (D). The top panels show images of representative cells on the gp120+ICAM-1 bilayer, and the bottom panels show images of representative cells on the ICAM-1 bilayer from one out of three independent experiments. Average and integrated fluorescence intensities acquired by TIRFM are plotted in the right and left graphs, respectively. A total of 30 to 300 cells were quantified for each condition. Bars = 5 μm.

after treatment with the Lck inhibitor, an ~1.5-fold increase in F-actin integrated fluorescence intensity was observed in the gp120-positive area compared to control (Fig. 8C). In contrast, the F-actin levels measured in the whole cell decreased by 2.5-fold compared to the control (Fig. 8D), showing that the lack of Lck-mediated signaling resulted in less actin polymerization at the VS. Taken together, these results indicate that membrane-proximal signaling induced in the VS leads to actin polymerization while creating an F-actin-depleted zone.

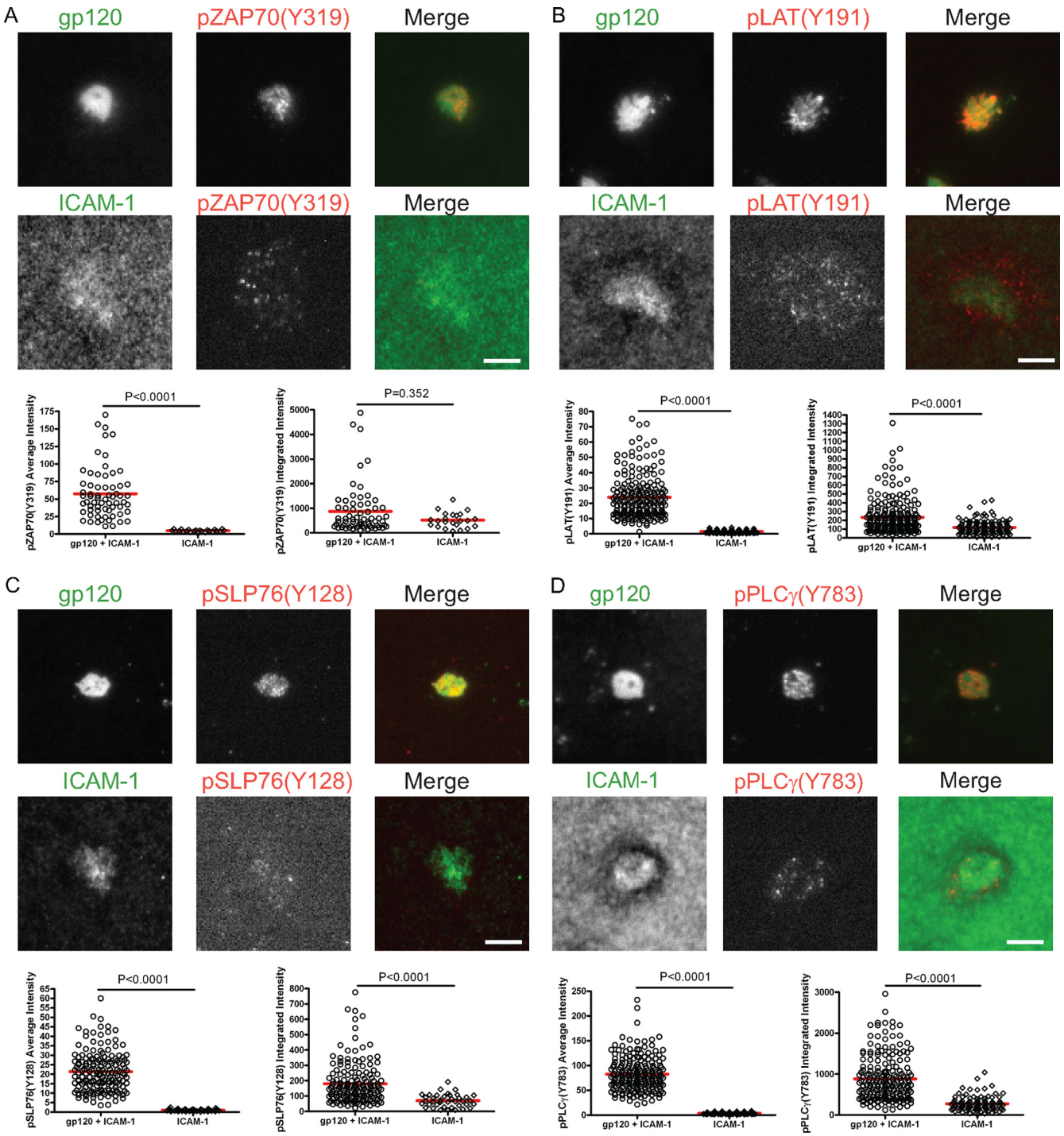

FIG. 5. Recruitment of TCR signaling machinery to the VS. CD4 T cells were allowed to interact with gp120+ICAM-1 or ICAM-1 bilayers for 45 min and then were fixed and stained with phospho-specific antibodies for pZAP70(Y319) (A), pLAT(Y191) (B), pSLP76(Y128) (C), and pPLCγ(Y783) (D). The top panels show a representative image of a cell on a gp120+ICAM-1 bilayer, and the bottom panels show a representative image of a cell on a ICAM-1 bilayer. Average and integrated fluorescence intensities acquired by TIRFM are depicted by the right and left graphs, respectively. A total of 30 to 200 cells were quantified for each condition. Data from one of three independent experiments with consistent results are shown.

DISCUSSION

We have shown previously that the interaction of uninfected target CD4 T cells with HIV-1 envelope gp120 and ICAM-1 on laterally mobile planar bilayers results in transient formation of VS, which share some common morphological features with the better defined IS. The present study provides the first molecular details about the initial assembly of VS, the local signaling triggered and the cytoskeleton organization underlying the VS. Similar to the TCR MCs found at the early stages of IS, the VS is initiated with gp120 MCs that converge cen-

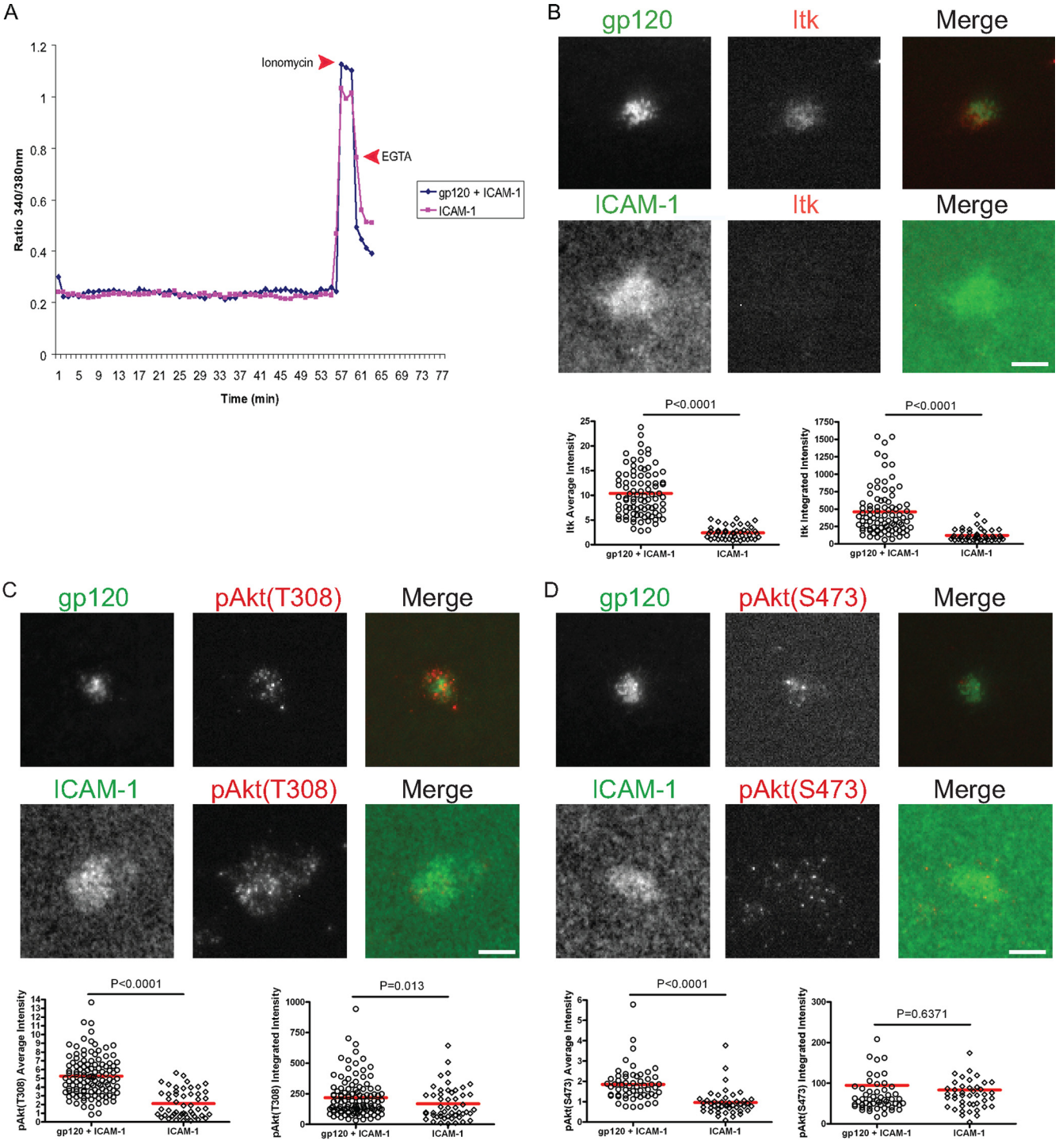

FIG. 6. Absence of canonical T-cell activation and incomplete prosurvival signals in the VS. (A) CD4 T cells were loaded with Ca^{2+}-sensitive dye Fura-2, introduced onto gp120+ICAM-1 or ICAM-1 bilayers, and imaged for up to 70 min. The ratio of the fluorescence intensity at 340 nm/fluorescence intensity at 380 nm was measured. The time points of ionomycin and EGTA injections are indicated by red arrowheads. (B to D) CD4 T cells were introduced onto the bilayers, and after 45 min, they were fixed and stained for Itk (B), pAkt(T308) (C), and pAkt(S473) (D). The top panels show representative images of cells on the gp120+ICAM-1 bilayer, and the bottom panels show representative images of cells on the ICAM-1 bilayer. Average and integrated fluorescence intensities from the TIRF channel are plotted in the left and right graphs, respectively. A total of 40 to 120 cells were quantified for each condition. Consistent findings were obtained in three independent experiments, and data from one experiment are shown. Bars = 5 μm.

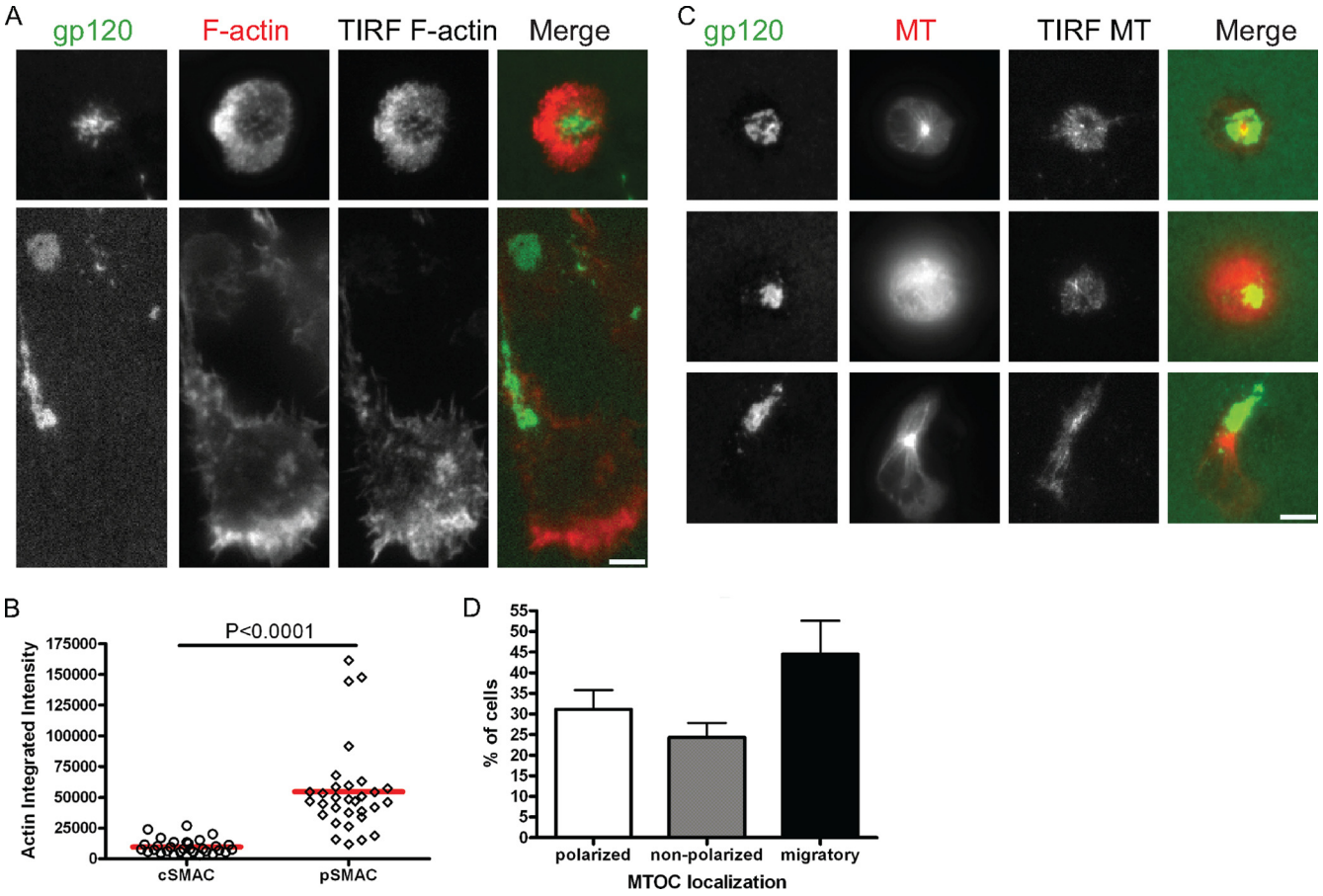

FIG. 7. VS-induced cytoskeletal rearrangements. (A) CD4 T cells were introduced onto gp120+ICAM-1 layers for 30 min, fixed, and stained with Alexa Fluor 568-phalloidin to detect F-actin. Representative images of F-actin staining detected in the wide-field and TIRF channels are shown. The top panels show the actin patterns in target cells forming VS, while the bottom panels show the actin patterns in migratory cells. Data from one out of two independent experiments are shown. (B) Integrated fluorescence intensity of actin staining in the VS cSMAC versus pSMAC (n = 30 cells). (C) CD4 T cells were introduced onto gp120+ICAM-1 bilayers for 30 min, fixed, and stained for β-tubulin to detect MTOC. Representative images of MT staining as detected in the wide-field and TIRF channels are shown. The top, middle, and bottom panels show MTOC polarized to the VS cSMAC, nonpolarized MTOC in a target cell, and MTOC at the uropod of a migratory cell, respectively. (D) The percentages of cells plus standard errors of the means (error bars) displaying different MTOC orientations are depicted. A total of 100 cells were analyzed in each experiment. Bars = 5 μm.

tripetally to form the cSMAC. As in the IS, the formation and centripetal transport of the gp120 MCs are actin dependent, as they are sensitive to inhibitors of actin polymerization. Unlike the TCR MCs (71), once formed, gp120 MCs remain actin dependent, although similar to the IS cSMAC (71), the VS cSMAC is actin independent. In addition to being a domain where virus antigens and cellular receptors are highly concentrated, one notable feature of the VS cSMAC is the cortical actin rearrangement that creates an F-actin-depleted zone immediately beneath the cSMAC (Fig. 7), which can be important for postentry events. Previous studies in which F-actin was visualized at the VS in cell-cell systems lacked the resolution needed to evaluate F-actin clearance from a 2- to 3-μm-size cSMAC region (41, 61). Our data showing actin-depleted cSMACs are consistent with the idea recently presented by Liu et al. (51) suggesting that the interaction of CD4 T cells with gp120 triggers cytoskeleton reorganization where actin first polymerizes to form a cortical F-actin zone and then depolymerizes so an F-actin-depleted zone is formed underneath the gp120-rich region. This model provides an explanation for the seemingly contradictory roles of F-actin in HIV infection: cortical actin polymerization is essential for the initial assembly of the VS and for the capping process of virus receptors (3, 40) that facilitates viral transfer and binding to the target CD4 T cells, but a zone depleted of cortical F-actin is then needed to enable the virus core to move from the plasma membrane to the nucleus. Nevertheless, the postentry steps in HIV-1 infection affected by cortical F-actin and its inhibitory mechanisms are still unknown. It is plausible that HIV-1 evolves to exploit the molecular segregation and signaling as induced physiologically in the IS for creating an actin-depleted zone in the VS cSMAC and possibly relieving postentry blocks.

Our model would suggest that HIV Gag should accumulate to induce viral budding opposite the F-actin-depleted cSMAC in the target cell. However, the exact localization of virus budding and entry in the context of the VS substructures (i.e., cSMAC versus pSMAC) remains unclear and should be fur-

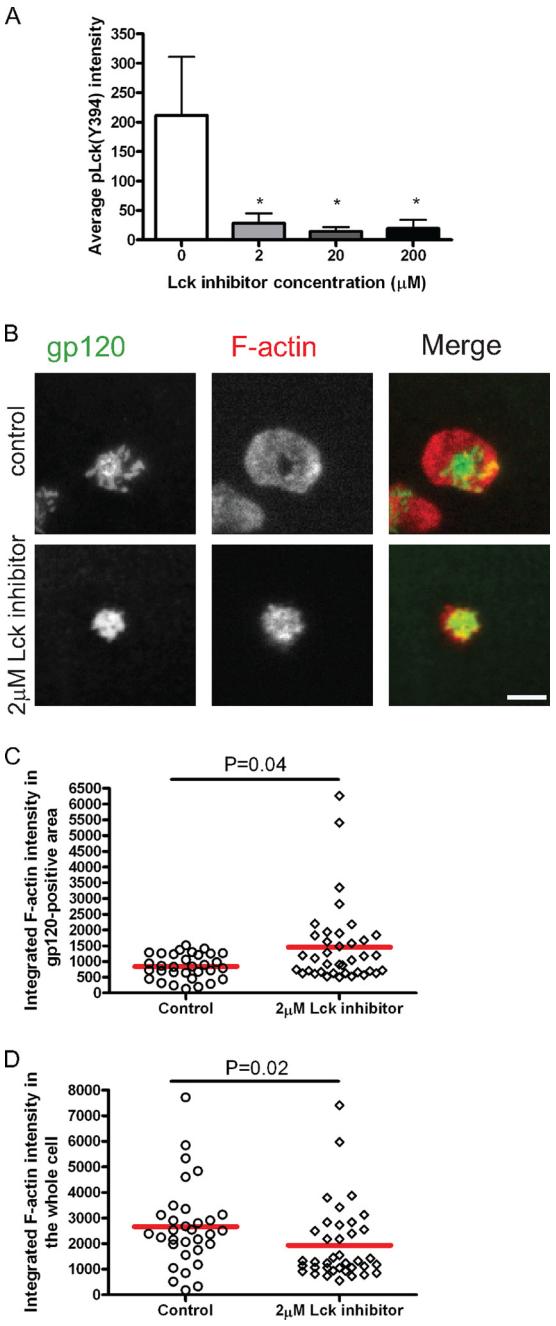

FIG. 8. Lck signaling is required for F-actin rearrangements in the VS. CD4 T cells were pretreated with the indicated concentrations of the Lck inhibitor or with DMSO (control) and then introduced onto gp120+ICAM-1 bilayers in the presence of the inhibitor. (A) After 30 min, the cells were fixed and stained with antibody specific for pLck(Y394). The fluorescence intensity detected by TIRFM was measured, and the average values plus standard deviations (error bars) are presented. Data from one out of two independent experiments are shown. Values that were significantly different ($P < 0.0001$) from the control values are indicated (*). (B and C) CD4 T cells pretreated with 2 μM of Lck inhibitor or DMSO only were introduced onto gp120+ICAM-1 bilayers for 30 min, fixed, and stained with Alexa Fluor 568-phalloidin to detect F-actin (B). Integrated fluorescence intensity of F-actin as detected by TIRFM was measured and calculated for gp120-positive area (C) and for the whole cell (D). Data from one out of three independent experiments are shown. Bar s= 5 μm.

ther investigated. In one study, Gag was reported to accumulate in a ring-shaped structure (61) that resembles a pSMAC, while in another study, it was shown to be in micrometer-sized buttons (36) that resemble the cSMAC. It is also not clear whether Gag and Env colocalize at the same substructures of VS, though they have been suggested to colocalize at the plasma membranes of virus-infected cells (34) and at the VS interface (41). Furthermore, viral transfer across the VS has been suggested to occur via endocytosis (8, 36), and cell-free virions have also been found to enter cells via fusion with endosomal membranes in a dynamin-dependent mechanism (55). Nevertheless, the IS cSMAC is a site of bidirectional membrane traffic (50) despite being relatively F-actin depleted (43, 68). Therefore, if virions are to be endocytosed at the cSMAC prior to fusion, it is likely that there is a sufficient F-actin level in the VS cSMAC to mediate this process while also allowing movement of the virus core to the nucleus.

The molecular basis for the formation of the F-actin-depleted zone underneath the VS cSMAC is not fully understood, though activation of Lck is clearly required for its formation (Fig. 8). A recent study by Yoder et al. (74) demonstrates that gp120 interaction with CXCR4 activates cofilin, an actin-depolymerizing factor, which facilitates HIV-1 postentry replication events in resting T cells, which otherwise are refractory to HIV-1 infection. Cofilin is an important component for F-actin dynamics at the periphery of the IS (64) and may also play a role in F-actin depletion in the center of the IS (43). In the IS, full TCR signaling is terminated in the cSMAC, but it is possible that some partial signaling remains to form the F-actin-depleted central zone (11). Whether cofilin plays a role in creating the F actin-depleted zone in the VS is not known, and the signaling pathway connecting Lck activity and F-actin depolymerization remains to be determined. Nevertheless, our data provide clear evidence for active local membrane-proximal TCR signaling at the VS. Lck is associated with gp120 MCs and is activated within minutes after CD4 T cells contact gp120 on the bilayer.

Evidence for downstream activation of the TCR signaling pathway at the VS is presented by the activation and recruitment of CD3ζ, ZAP70, LAT, SLP76, Itk, and PLCγ. Jolly et al. have shown before that CD3ε was partially recruited to the interface in 15% of cells forming VSs and thus concluded that the TCR is not involved (41). However, it is well established that TIRFM is much more sensitive for detection of TCR than cell-cell imaging methods (10, 49). Indeed, our experiments showed relatively weak recruitment of CD3ε and αβTCR to the VS interface compared to CD3ζ. Either preassociation of CD4 and TCR (44) or induced association following CD4 clustering (54) could account for the observed recruitment of TCR components following CD4 engagement by gp120. Moreover, evidence for TCR-CKR physical association upon chemokine engagement (45) further strengthens the possibility that once gp120 binds to CD4 and CKR, the TCR-CD3 ITAMs may be recruited to the VS and become available for phosphorylation by Lck.

Nevertheless, full T-cell activation as classically triggered via TCR is not induced at the VS, as indicated by the absence of PKCθ recruitment, intracellular Ca^{2+} influx, and CD69 upregulation. In contrast, soluble gp120 and cell-free virions have been shown to induce Ca^{2+} influx in T cells in a CKR-depen-

dent manner (53). The organization of gp160 trimers on virions could activate signals through a specific cross-linking geometry that might not be generated by monomeric gp120 in the supported planar bilayers. The mechanism by which HIV-1 virions would induce signals that are not induced by gp120 in the planar bilayers is not clear. The organization of molecules in the VS may inhibit signals that are induced by engagement of CD4 and CKR, or the soluble gp120 in the earlier studies may contain some aggregates. It should be noted that in our planar bilayer system, the target cell engages only gp120 and ICAM-1, while HIV-1 virions can acquire host cell surface molecules like CD28, CD152, CD80, and CD86 (30, 31) that can interact with their ligands on the target cells and modulate T-cell activation together with the viral Env. In addition, gp120 can engage $\alpha 4\beta 7$ (1) and other CKRs on T cells and other types of cells (26), all of which may contribute directly or indirectly to Ca^{2+} influx detected in the T cells. Another possible reason is the use of activated CD4 T cells in our experiments compared to nonactivated CD4 T cells in the other studies. In the quiescent G_0-phase cells, robust activation signals are needed to release postentry blocks and allow integration (67), whereas in the G_1-phase resting cells, a subthreshold stimulus is sufficient to support infection, albeit at a reduced level compared to activated CD4 T cells (69).

Akt phosphorylation is also induced upon VS formation, but only at one of the two phosphorylation sites associated with Akt activation. PI3K has been shown to regulate HIV-1 replication following viral entry in CD4 T cells and to trigger Akt activation in response to soluble gp120 and cell-free virions (27). The PI3K/Akt pathway is known to be crucial for cell survival (12) and has also been implicated to play a key role in prolonging survival of target cells and replication of many viruses other than HIV-1 (39). However, it is yet to be determined whether the prosurvival PI3K/Akt pathway is triggered by the VS in a manner that promotes target cell survival and early HIV-1 replication events. Considering that gp120 interaction with the CKR has been shown to induce apoptosis in CD4 T cells (6, 7, 56, 70), induction of a prosurvival pathway by the VS may serve as a counter mechanism to protect the target cells from gp120-mediated apoptosis.

In conclusion, the VS is generated by the convergence of gp120 MCs into a cSMAC. TCR signaling is initiated in MC and is sustained in the cSMAC. The signaling does not lead to canonical T-cell activation and proliferation but marks an F-actin-depleted zone in the VS center and thus may play a critical role in removing the cytoskeletal barriers for viral entry and infection.

ACKNOWLEDGMENTS

This work was supported by NIH grants AI060503 (M.W.C.) and AI071815 (C.E.H.) and the Roadmap Nanomedicine Development Center award PN2EY016586 (M.L.D.).

We thank S. Vardhana for advice on imaging with the EM-CCD camera.

REFERENCES

1. **Arthos, J., C. Cicala, E. Martinelli, K. Macleod, D. Van Ryk, D. Wei, Z. Xiao, T. D. Veenstra, T. P. Conrad, R. A. Lempicki, S. McLaughlin, M. Pascuccio, R. Gopaul, J. McNally, C. C. Cruz, N. Censoplano, E. Chung, K. N. Reitano, S. Kottilil, D. J. Goode, and A. S. Fauci.** 2008. HIV-1 envelope protein binds to and signals through integrin alpha4beta7, the gut mucosal homing receptor for peripheral T cells. Nat. Immunol. **9:**301–309.
2. **Barda-Saad, M., A. Braiman, R. Titerence, S. C. Bunnell, V. A. Barr, and L. E. Samelson.** 2005. Dynamic molecular interactions linking the T cell antigen receptor to the actin cytoskeleton. Nat. Immunol. **6:**80–89.
3. **Barrero-Villar, M., J. R. Cabrero, M. Gordon-Alonso, J. Barroso-Gonzalez, S. Alvarez-Losada, M. A. Munoz-Fernandez, F. Sanchez-Madrid, and A. Valenzuela-Fernandez.** 2009. Moesin is required for HIV-1-induced CD4-CXCR4 interaction, F-actin redistribution, membrane fusion and viral infection in lymphocytes. J. Cell Sci. **122:**103–113.
4. **Berg, L. J., L. D. Finkelstein, J. A. Lucas, and P. L. Schwartzberg.** 2005. Tec family kinases in T lymphocyte development and function. Annu. Rev. Immunol. **23:**549–600.
5. **Bhaskar, P. T., and N. Hay.** 2007. The two TORCs and Akt. Dev. Cell **12:**487–502.
6. **Biard-Piechaczyk, M., V. Robert-Hebmann, V. Richard, J. Roland, R. A. Hipskind, and C. Devaux.** 2000. Caspase-dependent apoptosis of cells expressing the chemokine receptor CXCR4 is induced by cell membrane-associated human immunodeficiency virus type 1 envelope glycoprotein (gp120). Virology **268:**329–344.
7. **Blanco, J., J. Barretina, B. Clotet, and J. A. Este.** 2004. R5 HIV gp120-mediated cellular contacts induce the death of single CCR5-expressing CD4 T cells by a gp41-dependent mechanism. J. Leukoc. Biol. **76:**804–811.
8. **Bosch, B., B. Grigorov, J. Senserrich, B. Clotet, J. L. Darlix, D. Muriaux, and J. A. Este.** 2008. A clathrin-dynamin-dependent endocytic pathway for the uptake of HIV-1 by direct T cell-T cell transmission. Antivir. Res. **80:**185–193.
9. **Bubeck Wardenburg, J., R. Pappu, J. Y. Bu, B. Mayer, J. Chernoff, D. Straus, and A. C. Chan.** 1998. Regulation of PAK activation and the T cell cytoskeleton by the linker protein SLP-76. Immunity **9:**607–616.
10. **Campi, G., R. Varma, and M. L. Dustin.** 2005. Actin and agonist MHC-peptide complex-dependent T cell receptor microclusters as scaffolds for signaling. J. Exp. Med. **202:**1031–1036.
11. **Cemerski, S., J. Das, E. Giurisato, M. A. Markiewicz, P. M. Allen, A. K. Chakraborty, and A. S. Shaw.** 2008. The balance between T cell receptor signaling and degradation at the center of the immunological synapse is determined by antigen quality. Immunity **29:**414–422.
12. **Chan, T. O., S. E. Rittenhouse, and P. N. Tsichlis.** 1999. AKT/PKB and other D3 phosphoinositide-regulated kinases: kinase activation by phosphoinositide-dependent phosphorylation. Annu. Rev. Biochem. **68:**965–1014.
13. **Chen, P., W. Hubner, M. A. Spinelli, and B. K. Chen.** 2007. Predominant mode of human immunodeficiency virus transfer between T cells is mediated by sustained Env-dependent neutralization-resistant virological synapses. J. Virol. **81:**12582–12595.
14. **Chirathaworn, C., S. A. Tibbetts, M. A. Chan, and S. H. Benedict.** 1995. Cross-linking of ICAM-1 on T cells induces transient tyrosine phosphorylation and inactivation of cdc2 kinase. J. Immunol. **155:**5479–5482.
15. **Cho, M. W., Y. B. Kim, M. K. Lee, K. C. Gupta, W. Ross, R. Plishka, A. Buckler-White, T. Igarashi, T. Theodore, R. Byrum, C. Kemp, D. C. Montefiori, and M. A. Martin.** 2001. Polyvalent envelope glycoprotein vaccine elicits a broader neutralizing antibody response but is unable to provide sterilizing protection against heterologous simian/human immunodeficiency virus infection in pigtailed macaques. J. Virol. **75:**2224–2234.
16. **Cicala, C., J. Arthos, N. Censoplano, C. Cruz, E. Chung, E. Martinelli, R. A. Lempicki, V. Natarajan, D. VanRyk, M. Daucher, and A. S. Fauci.** 2006. HIV-1 gp120 induces NFAT nuclear translocation in resting $CD4^+$ T-cells. Virology **345:**105–114.
17. **Cicala, C., J. Arthos, E. Martinelli, N. Censoplano, C. C. Cruz, E. Chung, S. M. Selig, D. Van Ryk, J. Yang, S. Jagannatha, T. W. Chun, P. Ren, R. A. Lempicki, and A. S. Fauci.** 2006. R5 and X4 HIV envelopes induce distinct gene expression profiles in primary peripheral blood mononuclear cells. Proc. Natl. Acad. Sci. USA **103:**3746–3751.
18. **Cicala, C., J. Arthos, A. Rubbert, S. Selig, K. Wildt, O. J. Cohen, and A. S. Fauci.** 2000. HIV-1 envelope induces activation of caspase-3 and cleavage of focal adhesion kinase in primary human $CD4^+$ T cells. Proc. Natl. Acad. Sci. USA **97:**1178–1183.
19. **Cicala, C., J. Arthos, M. Ruiz, M. Vaccarezza, A. Rubbert, A. Riva, K. Wildt, O. Cohen, and A. S. Fauci.** 1999. Induction of phosphorylation and intracellular association of CC chemokine receptor 5 and focal adhesion kinase in primary human $CD4^+$ T cells by macrophage-tropic HIV envelope. J. Immunol. **163:**420–426.
20. **Cicala, C., J. Arthos, S. M. Selig, G. Dennis, Jr., D. A. Hosack, D. Van Ryk, M. L. Spangler, T. D. Steenbeke, P. Khazanie, N. Gupta, J. Yang, M. Daucher, R. A. Lempicki, and A. S. Fauci.** 2002. HIV envelope induces a cascade of cell signals in non-proliferating target cells that favor virus replication. Proc. Natl. Acad. Sci. USA **99:**9380–9385.
21. **Davis, C. B., I. Dikic, D. Unutmaz, C. M. Hill, J. Arthos, M. A. Siani, D. A. Thompson, J. Schlessinger, and D. R. Littman.** 1997. Signal transduction due to HIV-1 envelope interactions with chemokine receptors CXCR4 or CCR5. J. Exp. Med. **186:**1793–1798.
22. **Del Corno, M., Q. H. Liu, D. Schols, E. de Clercq, S. Gessani, B. D. Freedman, and R. G. Collman.** 2001. HIV-1 gp120 and chemokine activation of Pyk2 and mitogen-activated protein kinases in primary macrophages me-

diated by calcium-dependent, pertussis toxin-insensitive chemokine receptor signaling. Blood **98:**2909–2916.
23. **Dimitrov, D. S., R. L. Willey, H. Sato, L. J. Chang, R. Blumenthal, and M. A. Martin.** 1993. Quantitation of human immunodeficiency virus type 1 infection kinetics. J. Virol. **67:**2182–2190.
24. **Dustin, M. L.** 2008. T-cell activation through immunological synapses and kinapses. Immunol. Rev. **221:**77–89.
25. **Dustin, M. L., and T. A. Springer.** 1988. Lymphocyte function-associated antigen-1 (LFA-1) interaction with intercellular adhesion molecule-1 (ICAM-1) is one of at least three mechanisms for lymphocyte adhesion to cultured endothelial cells. J. Cell Biol. **107:**321–331.
26. **Edinger, A. L., J. E. Clements, and R. W. Doms.** 1999. Chemokine and orphan receptors in HIV-2 and SIV tropism and pathogenesis. Virology **260:**211–221.
27. **François, F., and M. E. Klotman.** 2003. Phosphatidylinositol 3-kinase regulates human immunodeficiency virus type 1 replication following viral entry in primary $CD4^+$ T lymphocytes and macrophages. J. Virol. **77:** 2539–2549.
28. **Freiberg, B. A., H. Kupfer, W. Maslanik, J. Delli, J. Kappler, D. M. Zaller, and A. Kupfer.** 2002. Staging and resetting T cell activation in SMACs. Nat. Immunol. **3:**911–917.
29. **Geiger, B., D. Rosen, and G. Berke.** 1982. Spatial relationships of microtubule-organizing centers and the contact area of cytotoxic T lymphocytes and target cells. J. Cell Biol. **95:**137–143.
30. **Giguère, J. F., S. Bounou, J. S. Paquette, J. Madrenas, and M. J. Tremblay.** 2004. Insertion of host-derived costimulatory molecules CD80 (B7.1) and CD86 (B7.2) into human immunodeficiency virus type 1 affects the virus life cycle. J. Virol. **78:**6222–6232.
31. **Giguere, J. F., J. Diou, J. Madrenas, and M. J. Tremblay.** 2005. Virus attachment and replication are promoted after acquisition of host CD28 and CD152 by HIV-1. J. Infect. Dis. **192:**1265–1268.
32. **Goldberg, D. R., T. Butz, M. G. Cardozo, R. J. Eckner, A. Hammach, J. Huang, S. Jakes, S. Kapadia, M. Kashem, S. Lukas, T. M. Morwick, M. Panzenbeck, U. Patel, S. Pav, G. W. Peet, J. D. Peterson, A. S. Prokopowicz III, R. J. Snow, R. Sellati, H. Takahashi, J. Tan, M. A. Tschantz, X. J. Wang, Y. Wang, J. Wolak, P. Xiong, and N. Moss.** 2003. Optimization of 2-phenylaminoimidazo[4,5-h]isoquinolin-9-ones: orally active inhibitors of lck kinase. J. Med. Chem. **46:**1337–1349.
33. **Gomez, T. S., and D. D. Billadeau.** 2008. T cell activation and the cytoskeleton: you can't have one without the other. Adv. Immunol. **97:**1–64.
34. **Hermida-Matsumoto, L., and M. D. Resh.** 2000. Localization of human immunodeficiency virus type 1 Gag and Env at the plasma membrane by confocal imaging. J. Virol. **74:**8670–8679.
35. **Holdorf, A. D., K. H. Lee, W. R. Burack, P. M. Allen, and A. S. Shaw.** 2002. Regulation of Lck activity by CD4 and CD28 in the immunological synapse. Nat. Immunol. **3:**259–264.
36. **Hubner, W., G. P. McNerney, P. Chen, B. M. Dale, R. E. Gordon, F. Y. Chuang, X. D. Li, D. M. Asmuth, T. Huser, and B. K. Chen.** 2009. Quantitative 3D video microscopy of HIV transfer across T cell virological synapses. Science **323:**1743–1747.
37. **Huppa, J. B., and M. M. Davis.** 2003. T-cell-antigen recognition and the immunological synapse. Nat. Rev. Immunol. **3:**973–983.
38. **Izzard, C. S., and L. R. Lochner.** 1976. Cell-to-substrate contacts in living fibroblasts: an interference reflexion study with an evaluation of the technique. J. Cell Sci. **21:**129–159.
39. **Ji, W. T., and H. J. Liu.** 2008. PI3K-Akt signaling and viral infection. Recent Patents Biotechnol. **2:**218–226.
40. **Jimenez-Baranda, S., C. Gomez-Mouton, A. Rojas, L. Martinez-Prats, E. Mira, R. Ana Lacalle, A. Valencia, D. S. Dimitrov, A. Viola, R. Delgado, A. C. Martinez, and S. Manes.** 2007. Filamin-A regulates actin-dependent clustering of HIV receptors. Nat. Cell Biol. **9:**838–846.
41. **Jolly, C., K. Kashefi, M. Hollinshead, and Q. J. Sattentau.** 2004. HIV-1 cell to cell transfer across an Env-induced, actin-dependent synapse. J. Exp. Med. **199:**283–293.
42. **Jolly, C., I. Mitar, and Q. J. Sattentau.** 2007. Requirement for an intact T-cell actin and tubulin cytoskeleton for efficient assembly and spread of human immunodeficiency virus type 1. J. Virol. **81:**5547–5560.
43. **Kaizuka, Y., A. D. Douglass, R. Varma, M. L. Dustin, and R. D. Vale.** 2007. Mechanisms for segregating T cell receptor and adhesion molecules during immunological synapse formation in Jurkat T cells. Proc. Natl. Acad. Sci. USA **104:**20296–20301.
44. **Krogsgaard, M., Q. J. Li, C. Sumen, J. B. Huppa, M. Huse, and M. M. Davis.** 2005. Agonist/endogenous peptide-MHC heterodimers drive T cell activation and sensitivity. Nature **434:**238–243.
45. **Kumar, A., T. D. Humphreys, K. N. Kremer, P. S. Bramati, L. Bradfield, C. E. Edgar, and K. E. Hedin.** 2006. CXCR4 physically associates with the T cell receptor to signal in T cells. Immunity **25:**213–224.
46. **Kupfer, A., G. Dennert, and S. J. Singer.** 1983. Polarization of the Golgi apparatus and the microtubule-organizing center within cloned natural killer cells bound to their targets. Proc. Natl. Acad. Sci. USA **80:**7224–7228.
47. **Lee, C., Q. H. Liu, B. Tomkowicz, Y. Yi, B. D. Freedman, and R. G. Collman.** 2003. Macrophage activation through CCR5- and CXCR4-mediated gp120-elicited signaling pathways. J. Leukoc. Biol. **74:**676–682.
48. **Lee, C., B. Tomkowicz, B. D. Freedman, and R. G. Collman.** 2005. HIV-1 gp120-induced TNF-α production by primary human macrophages is mediated by phosphatidylinositol-3 (PI-3) kinase and mitogen-activated protein (MAP) kinase pathways. J. Leukoc. Biol. **78:**1016–1023.
49. **Lee, K. H., A. D. Holdorf, M. L. Dustin, A. C. Chan, P. M. Allen, and A. S. Shaw.** 2002. T cell receptor signaling precedes immunological synapse formation. Science **295:**1539–1542.
50. **Liu, D., Y. T. Bryceson, T. Meckel, G. Vasiliver-Shamis, M. L. Dustin, and E. O. Long.** 2009. Integrin-dependent organization and bidirectional vesicular traffic at cytotoxic immune synapses. Immunity **31:**99–109.
51. **Liu, Y., N. V. Belkina, and S. Shaw.** 2009. HIV infection of T cells: actin-in and actin-out. Sci. Signal. **2:**pe23.
52. **McDonald, D., L. Wu, S. M. Bohks, V. N. KewalRamani, D. Unutmaz, and T. J. Hope.** 2003. Recruitment of HIV and its receptors to dendritic cell-T cell junctions. Science **300:**1295–1297.
53. **Melar, M., D. E. Ott, and T. J. Hope.** 2007. Physiological levels of virion-associated human immunodeficiency virus type 1 envelope induce coreceptor-dependent calcium flux. J. Virol. **81:**1773–1785.
54. **Mittler, R. S., S. J. Goldman, G. L. Spitalny, and S. J. Burakoff.** 1989. T-cell receptor-CD4 physical association in a murine T-cell hybridoma: induction by antigen receptor ligation. Proc. Natl. Acad. Sci. USA **86:**8531–8535.
55. **Miyauchi, K., Y. Kim, O. Latinovic, V. Morozov, and G. B. Melikyan.** 2009. HIV enters cells via endocytosis and dynamin-dependent fusion with endosomes. Cell **137:**433–444.
56. **Molina, L., M. Grimaldi, V. Robert-Hebmann, L. Espert, M. Varbanov, C. Devaux, C. Granier, and M. Biard-Piechaczyk.** 2007. Proteomic analysis of the cellular responses induced in uninfected immune cells by cell-expressed X4 HIV-1 envelope. Proteomics **7:**3116–3130.
57. **Monks, C. R., B. A. Freiberg, H. Kupfer, N. Sciaky, and A. Kupfer.** 1998. Three-dimensional segregation of supramolecular activation clusters in T cells. Nature **395:**82–86.
58. **O'Shea, J. J., J. A. Johnston, J. Kehrl, G. Koretzky, and L. E. Samelson.** 2001. Key molecules involved in receptor-mediated lymphocyte activation. *In* Current protocols in immunology. Chapter 11, unit 119A. Wiley Interscience, Hoboken, NJ.
59. **Pearce-Pratt, R., D. Malamud, and D. M. Phillips.** 1994. Role of the cytoskeleton in cell-to-cell transmission of human immunodeficiency virus. J. Virol. **68:**2898–2905.
60. **Porter, M., T. Schindler, J. Kuriyan, and W. T. Miller.** 2000. Reciprocal regulation of Hck activity by phosphorylation of Tyr(527) and Tyr(416). Effect of introducing a high affinity intramolecular SH2 ligand. J. Biol. Chem. **275:**2721–2726.
61. **Rudnicka, D., J. Feldmann, F. Porrot, S. Wietgrefe, S. Guadagnini, M. C. Prevost, J. Estaquier, A. Haase, N. Sol-Foulon, and O. Schwartz.** 2009. Simultaneous human immunodeficiency virus cell-to-cell transmission to multiple targets through polysynapses. J. Virol. **83:**6234–6246.
62. **Schmoranzer, J., M. Goulian, D. Axelrod, and S. M. Simon.** 2000. Imaging constitutive exocytosis with total internal reflection fluorescence microscopy. J. Cell Biol. **149:**23–32.
63. **Sedwick, C. E., M. M. Morgan, L. Jusino, J. L. Cannon, J. Miller, and J. K. Burkhardt.** 1999. TCR, LFA-1, and CD28 play unique and complementary roles in signaling T cell cytoskeletal reorganization. J. Immunol. **162:**1367–1375.
64. **Sims, T. N., T. J. Soos, H. S. Xenias, B. Dubin-Thaler, J. M. Hofman, J. C. Waite, T. O. Cameron, V. K. Thomas, R. Varma, C. H. Wiggins, M. P. Sheetz, D. R. Littman, and M. L. Dustin.** 2007. Opposing effects of PKCtheta and WASp on symmetry breaking and relocation of the immunological synapse. Cell **129:**773–785.
65. **Sourisseau, M., N. Sol-Foulon, F. Porrot, F. Blanchet, and O. Schwartz.** 2007. Inefficient human immunodeficiency virus replication in mobile lymphocytes. J. Virol. **81:**1000–1012.
66. **Sowinski, S., C. Jolly, O. Berninghausen, M. A. Purbhoo, A. Chauveau, K. Kohler, S. Oddos, P. Eissmann, F. M. Brodsky, C. Hopkins, B. Onfelt, Q. Sattentau, and D. M. Davis.** 2008. Membrane nanotubes physically connect T cells over long distances presenting a novel route for HIV-1 transmission. Nat. Cell Biol. **10:**211–219.
67. **Stevenson, M.** 2003. HIV-1 pathogenesis. Nat. Med. **9:**853–860.
68. **Stinchcombe, J. C., E. Majorovits, G. Bossi, S. Fuller, and G. M. Griffiths.** 2006. Centrosome polarization delivers secretory granules to the immunological synapse. Nature **443:**462–465.
69. **Unutmaz, D., V. N. KewalRamani, S. Marmon, and D. R. Littman.** 1999. Cytokine signals are sufficient for HIV-1 infection of resting human T lymphocytes. J. Exp. Med. **189:**1735–1746.
70. **Varbanov, M., L. Espert, and M. Biard-Piechaczyk.** 2006. Mechanisms of CD4 T-cell depletion triggered by HIV-1 viral proteins. AIDS Rev. **8:**221–236.
71. **Varma, R., G. Campi, T. Yokosuka, T. Saito, and M. L. Dustin.** 2006. T cell receptor-proximal signals are sustained in peripheral microclusters and terminated in the central supramolecular activation cluster. Immunity **25:**117–127.

72. **Vasiliver-Shamis, G., M. Tuen, T. W. Wu, T. Starr, T. O. Cameron, R. Thomson, G. Kaur, J. Liu, M. L. Visciano, H. Li, R. Kumar, R. Ansari, D. P. Han, M. W. Cho, M. L. Dustin, and C. E. Hioe.** 2008. Human immunodeficiency virus type 1 envelope gp120 induces a stop signal and virological synapse formation in noninfected $CD4^+$ T cells. J. Virol. **82:**9445–9457.
73. **Weissman, D., R. L. Rabin, J. Arthos, A. Rubbert, M. Dybul, R. Swofford, S. Venkatesan, J. M. Farber, and A. S. Fauci.** 1997. Macrophage-tropic HIV and SIV envelope proteins induce a signal through the CCR5 chemokine receptor. Nature **389:**981–985.
74. **Yoder, A., D. Yu, L. Dong, S. R. Iyer, X. Xu, J. Kelly, J. Liu, W. Wang, P. J. Vorster, L. Agulto, D. A. Stephany, J. N. Cooper, J. W. Marsh, and Y. Wu.** 2008. HIV envelope-CXCR4 signaling activates cofilin to overcome cortical actin restriction in resting CD4 T cells. Cell **134:**782–792.
75. **Yokosuka, T., K. Sakata-Sogawa, W. Kobayashi, M. Hiroshima, A. Hashimoto-Tane, M. Tokunaga, M. L. Dustin, and T. Saito.** 2005. Newly generated T cell receptor microclusters initiate and sustain T cell activation by recruitment of Zap70 and SLP-76. Nat. Immunol. **6:**1253–1262.
76. **Zhu, P., J. Liu, J. Bess, Jr., E. Chertova, J. D. Lifson, H. Grise, G. A. Ofek, K. A. Taylor, and K. H. Roux.** 2006. Distribution and three-dimensional structure of AIDS virus envelope spikes. Nature **441:**847–852.